APS physics

CHORUS

This is the accepted manuscript made available via CHORUS. The article has been published as:

Franck-Condon processes in pentacene monolayers revealed in resonance Raman scattering

Rui He, Nancy G. Tassi, Graciela B. Blanchet, and Aron Pinczuk

Phys. Rev. B **83**, 115452 — Published 29 March 2011

DOI: 10.1103/PhysRevB.83.115452

Franck-Condon Processes in Pentacene Monolayers Revealed in Resonance Raman Scattering

Rui He,[1] Nancy G. Tassi,[2] Graciela B. Blanchet,[3] and Aron Pinczuk[1,4]

[1]*Department of Physics, Columbia University, New York, New York 10027*
[2]*DuPont, Central Research and Development, Wilmington, Delaware 19880*
[3]*Nano-Terra, Cambridge, Massachusetts 02139*
[4]*Department of Applied Physics and Applied Mathematics, Columbia University, New York, New York 10027*

(Dated: February 3, 2011)

Franck-Condon processes in pentacene monolayers are revealed in resonance Raman scattering from intramolecular vibrations. The Raman intensities from a totally symmetric vibrational mode display resonance enhancement double-peaks when incident or scattered photon energies overlap the free exciton (FE) optical emission. The two resonances are of about equal strength. This remarkable symmetry in the resonance Raman profile suggests that Franck-Condon overlap integrals for the respective vibronic transitions have the same magnitude which could be explained by the small displacement of potential energy curves along the configuration coordinate upon the FE excitation. The interference between scattering amplitudes in the Raman resonance reveals quantum coherence of the symmetry-split states (Davydov doublet) of the lowest intrinsic singlet exciton in pentacene monolayers.

PACS numbers: 78.55.Kz, 81.07.Nb, 71.35.Aa

REVIEW COPY NOT FOR DISTRIBUTION

I. INTRODUCTION

Pentacene is a benchmark material in the large organic semiconductor family. There is growing interest in properties of pentacene monolayers. The few monolayer limit is also significant in field effect transistors that use pentacene ultra-thin films as active layers.[1,2] In organic semiconductors molecular vibrations should play an important role in electrical transport by assisting the charge transfer processes in hopping conduction and by limiting the coherent band-like conduction through electron(hole)-vibration coupling.[3–6] Transfer rates in charge transport depend on overlap integrals for vibronic transitions (Franck-Condon overlaps).[5,7,8] A Franck-Condon analysis is thus crucial to understanding the coupling between vibrational modes and charge carriers in organic semiconductor monolayers.

In this contribution we show that excitation profiles of resonance Raman scattering (RRS) in high quality pentacene monolayers offer key insights on Franck-Condon processes. The measured intensities are strongly enhanced at the 0-0 resonance, when the incident photon energy overlaps the optical emission band of free exciton (FE) which is the lowest energy singlet exciton with a small Bohr radius.[3] The Raman intensities are also strongly enhanced at the 1-0 resonance, when the scattered photon energy overlaps the FE energy. We observe a striking symmetry of nearly identical strength in the 0-0 and 1-0 resonance doublet. The finding reveals fundamental features of Franck-Condon interactions for the coupling between vibrational modes and optical excitons in organic monolayers.

The observed Franck-Condon Raman resonance doublets are interpreted within the framework of the Raman processes in Figs. 1(a) and (b).[9,10] The finding that 0-0 and 1-0 resonances have largely identical strength shows that the Franck-Condon overlaps for the processes in Figs. 1(a) and (b) are largely identical. This symmetry suggests that the shift ΔQ of the potential energy curves due to photoexcitation of FE is very small and consistent with a small local lattice deformation.[3]

The resonance enhancement profiles reveal an interference between the FE and its symmetry-split twin exciton that arises from inter-molecular interactions between the two translationally inequivalent molecules in the 2D unit cell of the pentacene monolayers (Davydov splitting).[4,11,12] This unexpected effect reveals that within the short exciton lifetime there is quantum coherence of the two states.[13–16] For bulk pentacene the Davydov doublet corresponds to exciton bands with polarizations $\parallel b$ and $\perp b$ axis[17] (the a and b axes form an angle $\gamma = 85^o$). In pentacene monolayers the a and b axes are almost perpendicular ($\gamma = 90 \pm 0.2^o$).[11,12] Therefore, the Davydov doublets in monolayers are linked to distinct exciton bands with polarizations along the a and b axes. The observation of interference between the doublet states seems to indicate that pentacene molecules orient non-uniformly in the a-b plane in the monolayer films.[14,15]

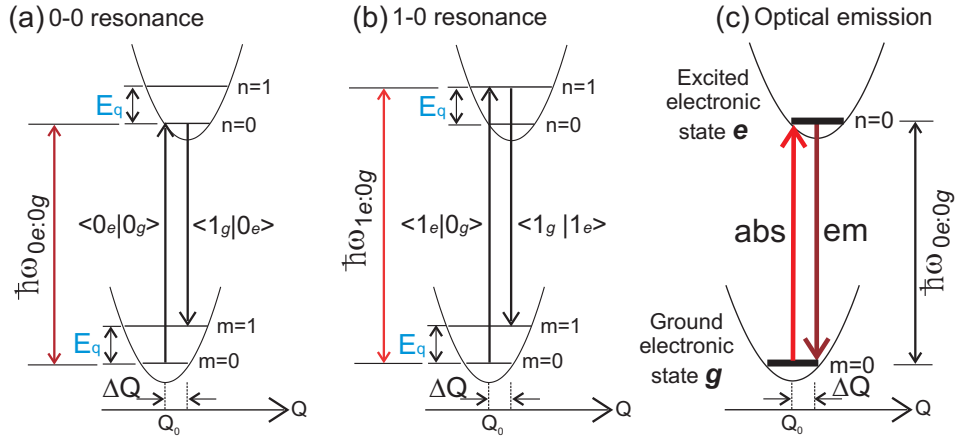

FIG. 1: (Color online)(a) and (b) Schematic illustration of resonance Raman scattering transitions in the Franck-Condon framework. Q is a configuration coordinate of the molecule. ΔQ is the displacement from ground state equilibrium upon excitation. The potential energy curves and vibrational levels (horizontal lines) are for one of the intra-molecular vibrational modes. E_q is the fundamental vibrational energy. (c) Schematic diagram of luminescence process when ΔQ is small. The up and down arrows represent optical absorption and emission processes. The thickened horizontal lines represent vibrational levels.

II. EXPERIMENT

We present data from two pentacene films with thicknesses of 1-monolayer (1ML) and 2-monolayer (2ML). The layers were thermally evaporated on a film of poly alpha-methylstyrene (PAMS) that serves as a compliant substrate. The inset on the right-hand side of Fig. 2(a) shows a schematic drawing of the configuration of the monolayers. The long axes of pentacene molecules are almost perpendicular to the substrate surface.[11] The monolayers display large islands with high uniformity within the micron length-scale. Details of sample preparation and characterization are described in Ref. [18]. Samples were mounted in a cryostat with windows for optical access. Because Raman lines from pentacene monolayers are much stronger and exciton bands are better defined at low temperatures, samples were cooled by cold helium gas to temperatures of ~10K. Similar results with larger experimental uncertainties would be obtained if measurements were conducted at higher temperatures. Linearly polarized dye and Ti:sapphire lasers with tuning range from 5700 to 8300Å were used. Incident laser power density was kept below $5W/cm^2$. The emitted and scattered light was dispersed by a Spex 1404 double spectrometer with holographic master gratings and CCD multichannel detection.

III. ANALYSIS AND DISCUSSION

Figures 2(a) and (b) show Raman spectra from intramolecular modes. The broad asymmetric band in each spectrum has two components whose contributions are obtained by decomposing Raman spectra into two peaks with fixed frequencies. The frequencies of the two components are almost the same in the two films studied. The lower energy mode at $\sim 1177cm^{-1}$=0.146eV is a symmetric (A_g) mode from in-plane bending of C-H bonds along the sides of pentacene molecules[10,19,20] (shown in the inset on the left of Fig. 2(a)). The weaker band at $\sim 1178cm^{-1}$ may arise from coupling between several molecules, and the origin and symmetry group of this band are still unclear.[20] We focus here on the resonance enhancement of the lower energy A_g mode which has relatively strong Raman intensity. Figure 2(c) shows Raman spectra from the 1ML sample excited by different photon energies.

Because the $1177cm^{-1}$ mode originates from the in-plane bending of C-H bonds along the sides of pentacene molecules, it may be more sensitive to neighboring molecules within the layer. The $1178cm^{-1}$ mode is attributed to the coupled modes between adjacent molecules.[20] The observation that these two modes are very similar in the 1ML and 2ML samples suggests that the in-plane structure and coupling are also very similar in the two films, consistent with the results obtained by X-ray diffractions.[12]. In contrast, the $1155cm^{-1}$ mode (shown in Ref. [18]) which arises from the vibrations of C-H bonds located at the outer rings of pentacene molecules is more sensitive to coupling between layers and it displays significant changes (splitting due to inter-layer interactions) when the number of layers changes from 1 to 2.

Figures 3(a) and (d) display profiles of resonance enhancements of Raman scattering intensities by the A_g modes at

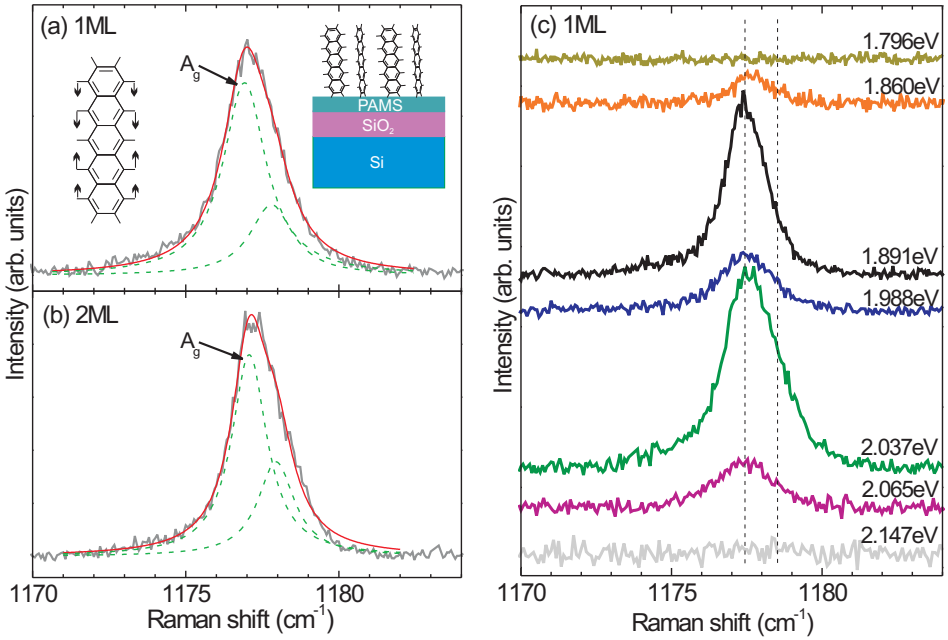

FIG. 2: (Color online)(a) and (b) Raman spectra from pentacene monolayers. The lower energy mode from each sample has A_g symmetry and is assigned to the in-plane bending of C-H bonds along the sides of the molecule (as shown in the left inset of (a)). The right inset in (a) is a schematic drawing of the configuration of a pentacene monolayer on PAMS. The drawing is not to scale. (c) Raman spectra from the 1ML film excited by different photon energies. All data are taken at T∼10K. The instrumental resolution is $0.8cm^{-1}$.

$\sim 1177cm^{-1}$ shown in Fig. 2. The intensities (in arbitrary units) are normalized to incident laser power, exposure time, and 4^{th} power of scattered photon frequency. The Raman enhancement profiles are doublets with nearly identical strength. The peaks at lower energy overlap the FE optical emission shown in Figs. 3(c) and (f). They are the 0-0 resonances with the FE state. The energy differences of the two resonances in both films, E_q=0.145±0.002eV, coincide almost exactly with the vibrational energy. This higher energy enhancement band is the 1-0 resonance. Both resonances exhibit red-shifts as the number of layers changes from 1 to 2, consistent with the red-shift of the FE band seen in luminescence. The widths of the 0-0 and 1-0 resonances, while slightly smaller, are comparable to that of the luminescence band.

The Raman scattering intensity I_s is written as[9,21]

$$I_s \propto \omega_s^4 V P_{vib}, \tag{1}$$

where ω_s is the scattered photon frequency, V is the scattering volume, and P_{vib} is the Raman scattering cross section. Within the Born-Oppenheimer approximation, the wave function is a product of electronic and vibrational terms. For totally symmetric (A_g) mode near resonance,[9,10,21]

$$P_{vib} \propto \left| \sum_{e,n_e} \frac{\langle g|\mathbf{M}|e\rangle\langle e|\mathbf{M}|g\rangle\langle m'_g|n_e\rangle\langle n_e|m_g\rangle}{\hbar\omega_{n_e:m_g} - \hbar\omega_{in} - i\Gamma_{n_e}} \right|^2, \tag{2}$$

where $|g\rangle$ and $|e\rangle$ are ground and excited states. m, m', and n are vibrational level indices. $\langle m'_g|n_e\rangle$ and $\langle n_e|m_g\rangle$ are Franck-Condon vibrational overlaps. $\hbar\omega_{in}$ is the incident photon energy, and Γ_{n_e} is the damping of the intermediate vibronic state $|n_e\rangle$. $\hbar\omega_{n_e:m_g}$ is the vibronic transition energy. $\langle\mathbf{M}\rangle$ is the electronic transition matrix element.

In the energy range of interest (1.8-2.1eV), the FE state and its higher energy Davydov counterpart (the DY state) which lies at 0.1eV above the FE[16,22] are the two main states that contribute to the resonance Raman processes in pentacene monolayers. Eq. (2) can thus be simplified as

$$\begin{aligned} P_{vib} \propto \Bigg| \sum_{k_{FE}} & \frac{\langle g|\mathbf{M}_{FE}|FE\rangle\langle FE|\mathbf{M}_{FE}|g\rangle\langle m'_g|k_{FE}\rangle\langle k_{FE}|m_g\rangle}{\hbar\omega_{k_{FE}:m_g} - \hbar\omega_{in} - i\Gamma_{k_{FE}}} \\ + \sum_{j_{DY}} & \frac{\langle g|\mathbf{M}_{DY}|DY\rangle\langle DY|\mathbf{M}_{DY}|g\rangle\langle m'_g|j_{DY}\rangle\langle j_{DY}|m_g\rangle}{\hbar\omega_{j_{DY}:m_g} - \hbar\omega_{in} - i\Gamma_{j_{DY}}} \Bigg|^2, \end{aligned} \tag{3}$$

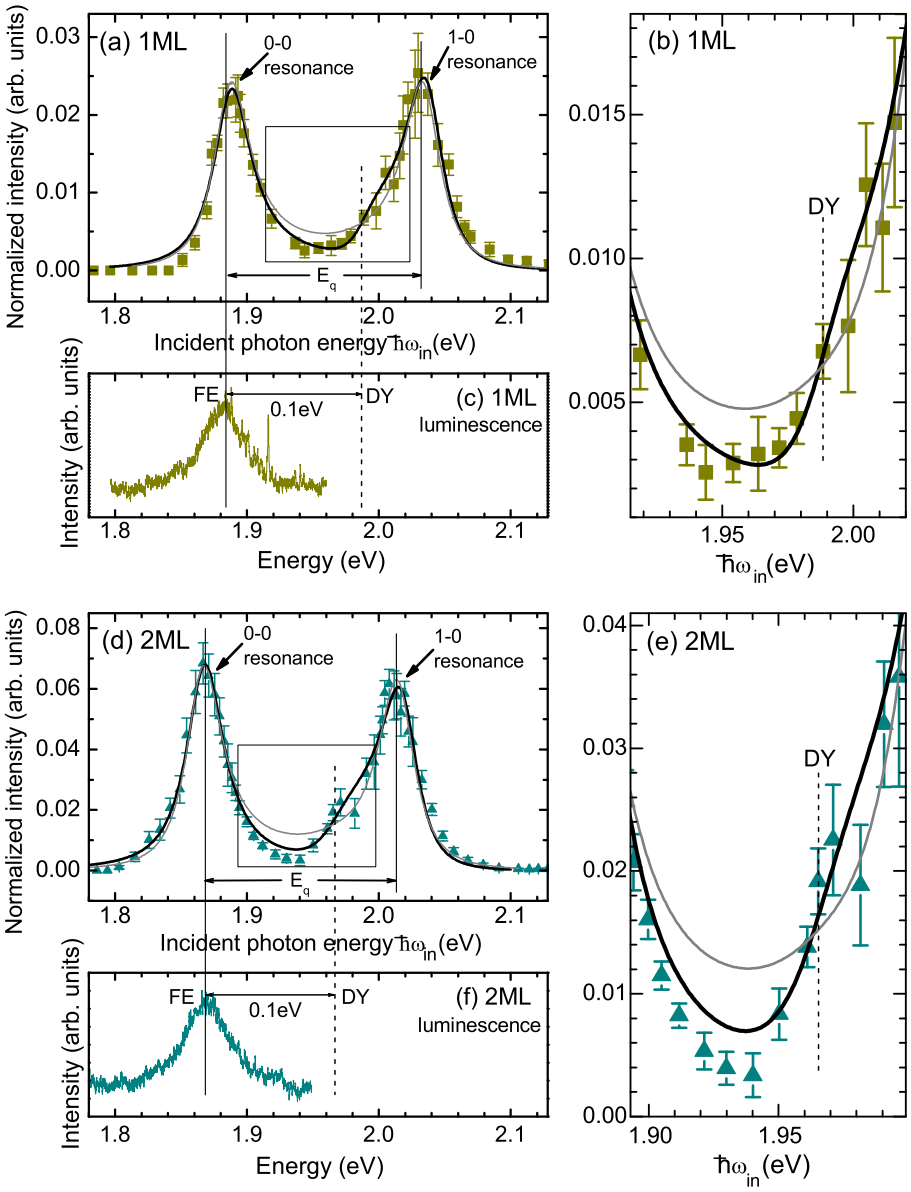

FIG. 3: (Color online)(a) The squares display Raman scattering intensities by the A_g mode at $\sim$1177cm^{-1} of the 1ML film. The black curve is a least-square fit of the resonance profile to Eq. (4). The grey line is a fit without quantum coherence of the FE and DY states. E_q is the energy of the vibrational mode. The solid vertical lines highlight the positions of the 0-0 and 1-0 resonances with the FE state. The dashed vertical line highlights the position of the higher energy Davydov component (DY) of the first singlet exciton state. (b) Expansion of the range in the box in panel (a). (c) FE luminescence spectrum from the 1ML sample. Luminescence from the DY state was not observed in this highly uniform pentacene monolayer grown on PAMS. (d)-(f) Same as in (a)-(c) for the 2ML film. All data are taken at T$\sim$10K.

where k and j are vibrational level indices at the FE and DY excitonic states, respectively. For the vibrational mode at 1177cm^{-1}(=0.146eV), only vibrational levels with indices 0 and 1 at the FE state and 0-th vibrational level at the DY state have significant contributions to Raman processes in the energy range of 1.8-2.1eV (see Figs. 3(a) and (d)).

TABLE I: Results from least-square fits of RRS profiles to Eq. (4). The parameter A is set to be -1, A', B, $\hbar\omega_{0_{DY}:0_g}$, and Γ_{DY} are adjustable parameters.

	1ML	2ML
A'	1.03±0.04	0.97±0.04
B	-0.3±0.12	-0.45±0.22
$\hbar\omega_{0_{DY}:0_g}$	1.988±0.006	1.967±0.006
$2\Gamma_{DY}$	0.037±0.011	0.05±0.011

Eq. (3) can be further simplified as

$$P_{vib} \propto \left| \frac{A}{\hbar\omega_{0_{FE}:0_g} - \hbar\omega_{in} - i\Gamma_{FE}} + \frac{A'}{\hbar\omega_{1_{FE}:0_g} - \hbar\omega_{in} - i\Gamma_{FE}} + \frac{B}{\hbar\omega_{0_{DY}:0_g} - \hbar\omega_{in} - i\Gamma_{DY}} \right|^2, \tag{4}$$

and the three numerators are

$$A \sim \langle g|\mathbf{M}_{FE}|FE\rangle\langle FE|\mathbf{M}_{FE}|g\rangle\langle 1_g|0_{FE}\rangle\langle 0_{FE}|0_g\rangle, \tag{5}$$

$$A' \sim \langle g|\mathbf{M}_{FE}|FE\rangle\langle FE|\mathbf{M}_{FE}|g\rangle\langle 1_g|1_{FE}\rangle\langle 1_{FE}|0_g\rangle, \tag{6}$$

$$B \sim \langle g|\mathbf{M}_{DY}|DY\rangle\langle DY|\mathbf{M}_{DY}|g\rangle\langle 1_g|0_{DY}\rangle\langle 0_{DY}|0_g\rangle. \tag{7}$$

The first and the second terms are for the 0-0 and 1-0 resonances with the FE state (shown in Figs. 1(a) and (b)). The third term is for the 0-0 resonance with the Davydov state (DY) at about 0.1eV above the FE. The 1-0 resonance with the DY state is not included in Eq. (4) because it occurs at much higher energy.

In Eqs. (2)-(4) Γ is linked to the lifetime of the exciton states. In this analysis we ignore the likely impact of inhomogeneous broadening of the exciton states. The reason is that for the bandwidth of the resonance profiles of 0.035-0.045eV (see Figs. 3(a) and (d)) we estimate exciton lifetimes in the range of 75-90fs which is consistent with those in optical pump probe measurements.[13,14]

The black lines in Fig. 3 display least-square fits of the resonance profiles with Eq. (4). In this analysis we set A=-1 and have four adjustable parameters A', B, $\hbar\omega_{0_{DY}:0_g}$, and Γ_{DY}. The agreement between the measured resonance profiles and the fits is good. It is significant that Eqs. (3) and (4) assumes there is interference (*i.e.* quantum coherence) between the scattering amplitude contributions of the FE and DY excitons in the Raman resonance. The grey lines in Fig. 3 show a fit of the resonance profiles without interference, in which the magnitude squares of the two contributions are added. The comparison between the fits reveals that the DY state prompts a weak Raman resonance that interferes with the two strong FE resonances by slightly distorting the resonance profiles around its energy position. The observed quantum coherence of the FE and DY doublet states, which correspond to the different polarizations along the a and b axes in the monolayer structures,[11,12,17] indicates that the orientation of pentacene molecules in the a-b plane is non-uniform.[3,4,14,15]

Table I summarizes the values of adjustable parameters obtained from fitting the RRS enhancement profiles. The position of the DY state (at $\hbar\omega_{0_{DY}:0_g}$) is highlighted by dashed vertical lines in Fig. 3. The parameter B that corresponds to the resonance with the DY state has the same sign as the parameter A and opposite sign as A'. The major impact of this DY resonance is in the region between the two FE resonances. For $\hbar\omega_{0_{FE}:0_g} < \hbar\omega_{in} < \hbar\omega_{0_{DY}:0_g}$ the DY resonance and the 0-0 resonance with the FE state interfere destructively because of the same sign of resonance numerators A and B. For $\hbar\omega_{0_{DY}:0_g} < \hbar\omega_{in} < \hbar\omega_{1_{FE}:0_g}$ the DY resonance interferes constructively with the 1-0 resonance with the FE state due to the opposite signs between parameters A' and B. The impact of these interferences is highlighted by the difference between the black and grey lines shown in Figs. 3(b) and (e).

The adjusted values of numerators A and A' differ merely in the sign, revealing that the respective Franck-Condon overlap integrals have the relation $\langle 1_g|0_{FE}\rangle\langle 0_{FE}|0_g\rangle = -\langle 1_g|1_{FE}\rangle\langle 1_{FE}|0_g\rangle$. This result implies that $\langle 1_g|0_{FE}\rangle = -\langle 1_{FE}|0_g\rangle$ and $\langle 0_{FE}|0_g\rangle = \langle 1_g|1_{FE}\rangle$. These are the symmetries of Franck-Condon coefficients that are revealed in the resonant Raman experiments. The symmetry is consistent with a small displacement ΔQ of potential energy curves shown in Fig. 1, implying that the local lattice deformation is very small upon the FE excitation.[3]

The magnitude of the numerator B is smaller than that of A, revealing a much weaker vibronic contribution from the higher Davydov component DY. Figure 4 shows an optical absorption spectrum from an 8ML(∼15nm)

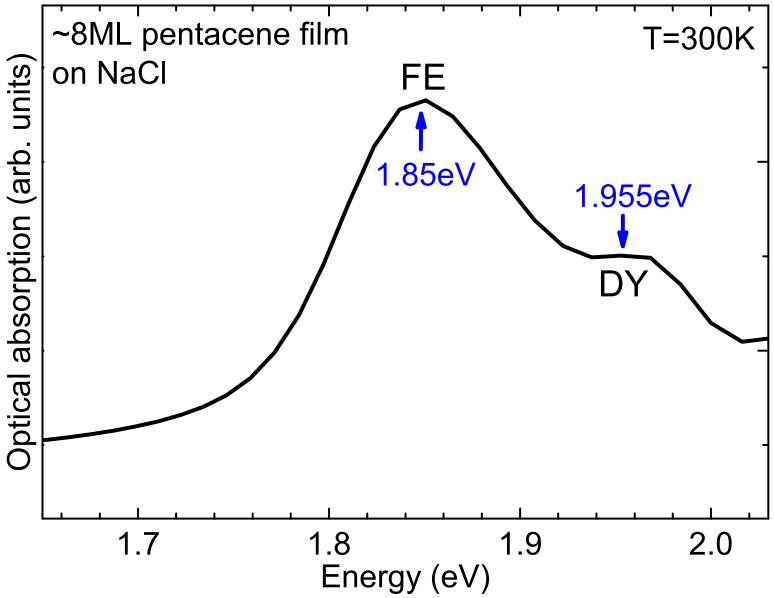

FIG. 4: (Color online) Optical absorption of a 8ML pentacene film on a transparent substrate NaCl. Data are at room temperature. Positions of the two Davydov bands are labeled.

pentacene film grown by the same method on a transparent substrate NaCl. The *a*-*b* in-plane structure of this film is presumably the same as those of the 1ML and 2ML films.[12] It is seen that the intensity of optical absorption of the higher Davydov component DY is much weaker than that of the lower energy counterpart. This suggests that vibronic coupling between the ground state and higher energy Davydov state is much weaker than that with the lower Davydov level, consistent with our identifications by resonance Raman method. Photoluminescence measurements from the 1ML and 2ML films show well-defined lower Davydov band FE, and the DY state is not observed. This is because excitons thermalize effectively to their lowest energy state FE before they optical recombine in these high quality monolayers.[23] A weak higher energy band DY of Davydov doublet is only observed in luminescence spectra of nanoscale cluster films, and it could be explained by nonequilibrium exciton recombination in which the higher energy DY excitons optically recombine before thermalization to the lower-lying FE state.[22]

IV. CONCLUSION

Raman scattering by a totally symmetric intramolecular vibration from pentacene monolayers reveals two major resonances with the FE state. The Franck-Condon overlap integrals of the two resonance terms that give rise to the 0-0 and 1-0 resonances have nearly the same magnitude with opposite signs. This anti-symmetry of the Franck-Condon overlaps could be linked to the small displacement of potential energy minimum along the configuration coordinate upon the FE excitation. The interference between scattering amplitudes in the Raman resonance reveals quantum coherence of the FE and DY states which are the Davydov doublets of the lowest singlet exciton in pentacene monolayers. RRS is demonstrated to be a versatile and convenient approach to explore exciton-vibration coupling in organic monolayers.

Acknowledgments

This work was supported primarily by the Nanoscale Science and Engineering Initiative of the National Science Foundation under NSF Award Number CHE-0641523, and by the New York State Office of Science, Technology, and Academic Research (NYSTAR).

[1] R. Ruiz, A. Papadimitratos, A. C. Mayer, and G. G. Malliaras, Adv. Mater. **17**, 1795 (2005).
[2] A. Shehu, S. D. Quiroga, P. D'Angelo, C. Albonetti, F. Borgatti, M. Murgia, A. Scorzoni, P. Stoliar, and F. Biscarini, Phys. Rev. Lett. **104**, 246602 (2010).
[3] E. A. Silinsh and V. Capek, Organic Molecular Crystals, AIP Press, New York, USA (1994).
[4] M. Pope and C. E. Swenberg, Electronic Processes in Organic Crystals and Polymers, Oxford University Press, New York (1999).
[5] J. L. Brédas, D. Beljonne, V. Coropceanu, and J. Cornil, Chem. Rev. **104**, 4971 (2004).
[6] A. Troisi and G. Orlandi, J. Phys. Chem. A **110**, 4065 (2006).
[7] A. M. Kelley, J. Phys. Chem. A **103**, 6891 (1999).
[8] J. T. Hupp and R. D. Williams, Acc. Chem. Res. **34**, 808 (2001).
[9] D. A. Long, em The Raman Effect: A Unified Treatment of the Theory of Raman Scattering by Molecules, John Wiley & Sons Ltd., England (2002).
[10] Y. Yamakita, J. Kimura, and K. Ohno, J. Chem. Phys. **126**, 064904 (2007).
[11] S. E. Fritz, S. M. Martin, C. D. Frisbie, M. D. Ward, and M. F. Toney, J. Am. Chem. Soc. **126**, 4084 (2004).
[12] R. Ruiz, A. C. Mayer, G. G. Malliaras, B. Nickel, G. Scoles, A. Kazimirov, H. Kim, R. L. Headrick, and Z. Islam, Appl. Phys. Lett. **85**, 4926 (2004).
[13] H. Marciniak, M. Fiebig, M. Huth, S. Schiefer, B. Nickel, F. Selmaier, and S. Lochbrunner, Phys. Rev. Lett. **99**, 176402 (2007).
[14] C. Jundt, G. Klein, B. Sipp, J. Le Moigne, M. Joucla, and A. A. Villaeys, Chem. Phy. Lett. **241**, 84 (1995).
[15] T. Jentzsch, H. J. Juepner, K.-W. Brzezinka, and A. Lau, Thin Solid Films **315**, 273 (1998).
[16] B. Fraboni, A. Scidà, A. Cavallini, P. Cosseddu, A. Bonfiglio, S. Milita, and M. Nastasi, Appl. Phys. Lett. **96**, 163302 (2010).
[17] T. Aoki-Matsumoto, K. Furuta, T. Yamada, H. Moriya, K. Mizuno, and A. H. Matsui, Int. J. of Modern Phys. B **15**, 3753 (2001).
[18] R. He, N. G. Tassi, G. B. Blanchet, and A. Pinczuk, Appl. Phys. Lett. **94**, 223310 (2009).
[19] H.-L. Cheng, Y.-S. Mai, W.-Y. Chou, and L.-R. Chang, Appl. Phys. Lett. **90**, 171926 (2007).
[20] I. Stenger, A. Frigout, D. Tondelier, B. Geffroy, R. Ossikovski, and Y. Bonnassieux, Appl. Phys. Lett. **94**, 133301 (2009).
[21] R. J. H. Clark and B. Stewart, J. Am. Chem. Soc. **103**, 6593 (1981).
[22] R. He, N. G. Tassi, G. B. Blanchet, and A. Pinczuk, Appl. Phys. Lett. **87**, 103107 (2005).
[23] R. He, N. G. Tassi, G. B. Blanchet, and A. Pinczuk, Appl. Phys. Lett. **96**, 263303 (2010).